Ecotoxicology and Environmental Safety 148 (2018) 601–607

Contents lists available at ScienceDirect

Ecotoxicology and Environmental Safety

journal homepage: www.elsevier.com/locate/ecoenv

Removal of anionic dyes (Reactive Black 5 and Congo Red) from aqueous solutions using Banana Peel Powder as an adsorbent

Venkata Subbaiah Munagapati[a], Vijaya Yarramuthi[b], Yeji Kim[a], Kwon Min Lee[a], Dong-Su Kim[a,*]

[a] Department of Environmental Science and Engineering, Ewha Womans University, 11-1 Daehyun-Dong, Seodaemun-Gu, Seoul 120-750, Republic of Korea
[b] Department of Chemistry, Vikrama Simhapuri University, Nellore 524003, Andhra Pradesh, India

ARTICLE INFO

Keywords:
Adsorption
Anionic dyes
Isotherms
Kinetics
Temperature
Thermodynamics

ABSTRACT

The adsorption characteristics of Reactive Black 5 (RB5) and Cong Red (CR) onto Banana Peel Powder (BPP) from aqueous solution were investigated as a function of pH, contact time, initial dye concentration and temperature. The BPP was characterized by Fourier Transform Infrared Spectroscopy (FTIR) and Scanning Electron Microscopy (SEM) analysis. FTIR results revealed that hydroxyl (–OH), amine (–NH) and carboxyl (–C=O) functional groups present on the surface of BPP. The SEM results show that BPP has an irregular and porous surface morphology which is adequate for dye adsorption. The equilibrium data were analyzed using Langmuir and Freundlich isotherm models. Experimental results were best represented by the Langmuir isotherm model. The adjustments of models were confirmed by the Chi-square (χ^2) test and the correlation coefficients (R^2). The maximum monolayer adsorption capacities of RB5 and CR on BPP calculated from Langmuir isotherm model were 49.2 and 164.6 mg/g at pH 3.0 and 298 K. Experimental data were also tested in terms of adsorption kinetics using pseudo-first-order and pseudo-second-order kinetic models. The results showed that the adsorption processes of both RB5 and CR followed well pseudo-second-order kinetic models. The calculated thermodynamic parameters ΔG°, ΔH° and ΔS° showed that the adsorption of RB5 and CR onto BPP was feasible, spontaneous and endothermic in the temperature range 298–318 K. The RB5 and CR were desorbed from BPP using 0.1 M NaOH. The recovery for both anionic dyes was found to be higher than 90%. Based on these it can be concluded that BPP can be used as an effective, low cost, and eco-friendly adsorbent for CR removal than RB5 from aqueous solution.

1. Introduction

Water pollution due to the release of various toxic chemicals from industrialization and urbanization is a global problem. Among the various notorious toxic chemicals, dyes, metals, organics and pharmaceuticals are highly concerned (Karthikeyan et al., 2012; Saleh and Gupta, 2011, 2012a, 2012b, 2012c, 2014; Mohammadi et al., 2011; Gupta et al., 2011a, 2011b, 2012a, 2012b, 2012c, 2013; Gupta and Nayak, 2012; Gupta and Saleh, 2013; Jain et al., 2003; Mittal et al., 2009a, 2009b, 2010a, 2010b; Khani et al., 2010; Saravanan et al., 2013a, 2013b, 2013c, 2013d, 2013e, 2013f, 2014a, 2014b, 2014c, 2015a, 2015b, 2015c, 2015d, 2016; Devaraj et al., 2016; Ahmaruzzaman and Gupta, 2011; Rajendran et al., 2016). The large quantities of colored effluent discharged from textile, leather, paper, plastic, cosmetics, food and mineral processing industries has become a significant environment problem (Chatterjee et al., 2011). The disposal of wastewater containing industrial dyes into rivers and lakes without proper treatment has caused many problems. Some dyes have mutagenic, carcinogenic or teratogenic properties, in addition to colouring the body of water, because of which algae and phytoplankton in lakes and rivers are also adversely affected. Furthermore, the improper wastewater disposal leads to promotion of disturbances in gas solubility, causing damage to the tills of aquatic organisms and disrupting their spawning sites and refuges (Elisandra do Nascimento et al., 2015). Therefore, it is important to treat colored effluents for the removal of dyes. Dyes can be classified as anionic (acid, direct and reactive dyes), cationic (basic dyes) and nonionic (disperse dyes) dyes according to their dissociation in an aqueous solution. Azo dyes, (write cationic/anionic) generally possess one or more azo bonds (–N=N–), these are heavily utilized in the textile and several food industries.

Several conventional methods are available for color removal from wastewater, such as membrane separation (Ciardelli et al., 2000), chemical oxidation (Swaminathan et al., 2003), electrocoagulation (Alinsafi et al., 2004), adsorption (Mall et al., 2005) and coagulation and flocculation (Panswed and Wongchaisuwan, 1986). Most of these methods have certain limitations in their applications, for example,

* Corresponding author.
E-mail address: dongsu@ewha.ac.kr (D.-S. Kim).

https://doi.org/10.1016/j.ecoenv.2017.10.075
Received 2 August 2017; Received in revised form 23 October 2017; Accepted 31 October 2017

very harsh reaction conditions, high cost and secondary pollution. From the viewpoint of sustainable development and comprehensive utilization of resources, adsorption has a promising prospect and a wide range of applications due to its high removal efficiency, low cost, mild operating conditions, no secondary pollution and good performance over other conventional treatment processes in the removal of dyes from waste water.

Many sorbents based on low-cost agricultural by-products had been used for dye sorption from wastewater, which included mandarin peels (Pavan et al., 2007), wood apple shell (Jain and Jayaram, 2010), green coconut fibers (Cristovao et al., 2011), grape fruit peels (Saeed et al., 2010), peanut hull (Gong et al., 2005), peat (Allen et al., 2004) rice husk (Han et al., 2008) wood sawdust (Jain and Sikarwar, 2008), peanut husk (Sadaf and Bhatti, 2014), pine sawdust (Ozacar and Sengil, 2005), banana peel and green coconut mesocrap (Nascimento et al., 2015), electrocoagulation/banana peel (Carvalho et al., 2015), Banana peel-activated carbon (Ma et al., 2015) and orange peel (Arami et al., 2005). As one of the most consumed fruits in the world, banana is a very common fruit. Banana peel is the main residue, corresponding to 30–40% (w/w), and has been mainly used in composting, animal feeding and the production of proteins, methane, ethanol, pectin and enzymes (Silva et al., 2013). Cellulose, pectin, chlorophyll, and other low molecular weight species are its main constituents. Various chemical groups exist on the banana peel surface, including carboxyl, hydroxyl and amide groups, which have been extensively proven to play a critical role in the adsorption processes (e.g. enhancing sorption capacity and shortening stable time) (Mohammed and Chong, 2014). Banana peel contains lipids (1.7%), proteins (0.9%), crude fiber (31%) and carbohydrates (59%). The various minerals present are potassium (78.10 mg/g), manganese (76.20 mg/g), sodium (24.30 mg/g), calcium (19.20 mg/g) and iron (0.61 mg/g). Preliminary investigations show that several tones of banana peels are produced daily in market places and household garbage, creating an environmental nuisance and disposal problem. Reuse of banana peel as adsorbent is an interesting way to solve this problem. It is an abandoned, readily available, low-cost and cheap, environment friendly bio-material. Considering the above criteria, banana peel was chosen as an adsorbent for the removal of anionic dyes from aqueous solutions.

RB5 and CR are the well known anionic azo dyes which are soluble in water. The sulfonic acid groups present in them made them to exist in anionic nature. Therefore one can expect the same type of adsorption for the two dyes on an adsorbent or CR showing more adsorption than RB5 on BPP. This investigation gave us the real or experimental adsorption trend of the two dyes on BPP. The objective of the present work is to investigate the adsorption potential of BPP as an alternative adsorbent material for RB5 and CR removal from aqueous solution. The study includes an evaluation of the effects of various process parameters such as pH, contact time, initial dye concentration and temperature. The adsorption kinetic data was tested by pseudo-first-order and pseudo-second-order kinetic models. The equilibrium data were analyzed using Langmuir and Freundlich isotherm models. The results at different temperatures are used to evaluate thermodynamic parameters. In addition, Scanning Electron Microscopy (SEM) was used to identify the morphological structure of BPP and Fourier Transform Infrared (FTIR) spectroscopy was employed to elucidate the adsorption mechanism.

2. Materials and methods

2.1. Preparation of adsorbent

Bananas were purchased from a local market, Seoul, Korea. The Banana Peels were thoroughly washed with distilled water to remove surface dirt and adhering impurities, cut into small pieces, crushed and sieved in a mesh size 150 μm size by standard sieves. The Banana Peel Powder dried in an air oven at 105 °C for 2 h until a constant weight was reached. After complete drying, the Banana Peel Powder was stored in air tied bottles for experimental uses.

2.2. Preparation of dye solution

Stock solutions (1000 mg/L) of dyes were prepared in deionized and double distilled water and diluted to get the desired concentration of dyes. Calibration curves for dyes were prepared by measuring the absorbance of different concentrations of the dyes.

2.3. Chemicals and equipment

All chemical used in this work, were of analytical reagent grade and were used without further purification. RB5 (≈55% dye content, M.W. = 991.80) and CR (≥35% dye content, M.W. = 991.82) were purchased from Sigma-Aldrich Korea Ltd. (Seoul, Korea). The structure of dyes is shown in Table S1. Double deionized water (Milli-Q Millipore 18.2 MΩ cm^{-1} conductivity) was used for all dilutions. A pH meter (pH-240 L, NEOMET, Korea) was used for pH measurements. The pH meter was calibrated using standard buffer solutions of pH 4.0, 7.0 and 10.0. Fourier Transform Infrared Spectrometer (BIO-RAD, FTS-135, USA) was used for the IR spectral studies (4000–400 cm^{-1}) of adsorbent. For IR spectral studies, 1 mg of sample was mixed and ground with 100 mg of KBr and made into pellet. The background absorbance was measured by suing pure KBr pellet. Scanning Electron Microscopy (JEOL, JSM-7600F, Japan) was used to study the morphological features of the adsorbent. The dye concentrations in the samples were analyzed using UV/Vis spectrophotometer (Optizen Pop, Korea). The wavelength was selected so as to obtain maximum absorbance for each dyestuff and the λ_{max} values are 597 nm and 497 nm for RB5 and CR, respectively.

2.4. Batch experimental procedure

Batch experiments were carried out in 50 mL falcon tubes at 25 °C to evaluate various parameters such as pH, contact time, initial dye concentration and temperature. The pH edge experiments were performed by mixing 30 mL solution of RB5 and CR concentration (300 mg/L) and 0.03 g of adsorbent in 50 mL of falcon tubes. The pH values of the solutions were adjusted in the range of 3–10 using 0.1 M HCl and 0.1 M NaOH solutions. All tubes were agitated in a shaker at 180 rpm and 25 °C for 24 h. After reaching equilibrium, the adsorbent was separated by means of centrifugation at 3000 rpm for 3 min. The remaining dye concentration was appropriately diluted with distilled water and analyzed using UV/Vis spectrophotometer.

The dye uptake (q) was calculated from the difference between the concentrations of RB5 and CR before and after sorption using the Eq. (1):

$$q = \frac{C_i V_i - C_f V_f}{M} \quad (1)$$

In this equation, C_i and C_f are the initial and final dye concentrations in the solution (mg/L), V_i and V_f are the initial and final (initial plus added HCl or NaOH solutions) solution volumes, and M is the mass of sorbent (g).

Adsorption isotherms of RB5 and CR were evaluated at different temperatures (298, 308 and 318 K) to measure the maximum sorption capacities of BPP. The initial concentration of RB5 and CR was varied from 50 to 300 mg/L, which resulted in different final dye concentrations after sorption equilibrium. Adsorption kinetic experiments were carried out using different RB5 and CR concentrations such as 50, 100 and 150 mg/L. The experimental procedure was the same as described in the pH edge experiments, except that the samples were collected at different time intervals to determine the attainment of sorption equilibrium. Other remaining procedures were the same as those used in the pH edge experiments.

2.5. Desorption studies

Desorption measurements were conducted in order to explore the feasibility of recovering both the dye and the adsorbent. For this purpose, 0.03 g BPP saturated with RB5 and CR was removed from solution and transferred into 50 mL polypropylene centrifuge tubes, to this 30 mL of deionized water, 0.1 M HCl, 0.1 M CH_3COOH and 0.1 M NaOH (one at one time) was added and the tubes were agitated in a multi-shaking incubator at 180 rpm and 25 °C for 24 h. The desorbed dye concentration was analyzed using UV/Vis spectrophotometer and desorption efficiency was calculated as follows:

$$Desorption\ efficiency = \frac{Amount\ of\ dye\ desorbed}{Amount\ of\ dye\ adsorbed} \times 100 \quad (2)$$

3. Results and discussion

3.1. Characterization of BPP

The FTIR spectra of BPP, RB5 loaded BP and CR loaded BPP in the range of 4000–400 cm^{-1} were recorded and compared with each other to obtain information on the nature of the possible adsorbent-dye ion interactions. They are presented in Fig. 1. The peak at 3376 cm^{-1} was due to bounded hydroxyl (–OH) or amine (–NH) groups. The peaks observed at 2920 cm^{-1} can be assigned to the –CH group. The peaks at 1735 cm^{-1} were attributed to stretching vibration of carboxyl group (–C=O). The peaks at 1615 and 1445 cm^{-1} were attributed to stretching vibration of carboxyl group. The bands observed at 1103 and 1055 cm^{-1} assigned to alcoholic C-O and C-N stretching vibration respectively, thus showing the presence of hydroxyl and amine groups on the adsorbent surface. The spectra of the RB5 and CR loaded BPP showed similar characteristics as the BPP except for slight changes. The FTIR spectrum of the RB5 and CR loaded BPP indicates that the peaks are slightly shifted from their positions and the intensity gets altered. These results indicated the involvement of some functional groups (hydroxyl, amine and carboxyl) in the adsorption of RB5 and CR on the surface of BPP through weak electrostatic interaction or Van der Waals forces.

The banana peels, before and after adsorption were observed using Scanning Electron Microscopy. Fig. 2(A), show SEM of BPP before adsorption. The peel has an irregular and porous surface. The many pores on its surface support the adsorption process. Fig. 2(B) and (C) shows SEM of BPP after adsorption of RB5 and CR. The peel appears to have a rough surface with carter-like pores as they are partially covered by RB5 and CR. After adsorption, the pores became thicker and blocked with RB5 and CR.

3.2. Effect of pH

Solution pH plays an important role in controlling the surface charge of the adsorbent, the degree of ionization of the adsorbate in the solution as well as dissociation of various functional groups on the active sites of the adsorbent (Wawrzkiewicz and Hubicki, 2009). The effect of pH on the adsorption of RB5 and CR onto BPP was studied in the range of pH 3.0–10.0 and the results are given in Fig. 3. The maximum uptake of RB5 and CR occurred at pH 3.0 (26.9 and 146.7 mg/g for RB5 and CR, respectively) and then decreased as the pH increased from 3.0 to 10.0. This can be explained as in the aqueous solutions, the anionic dye exists in dissociated form as anionic dye ions:

$$Dye - SO_3Na \xrightarrow{Water} Dye - SO_3^- + Na^+ \quad (3)$$

Acidic conditions could be favorable for the adsorption between two dyes and the adsorbent, because a significantly high electrostatic force of attraction exists between the positively charged surfaces of the adsorbent and the negative charged anionic dye under acidic conditions

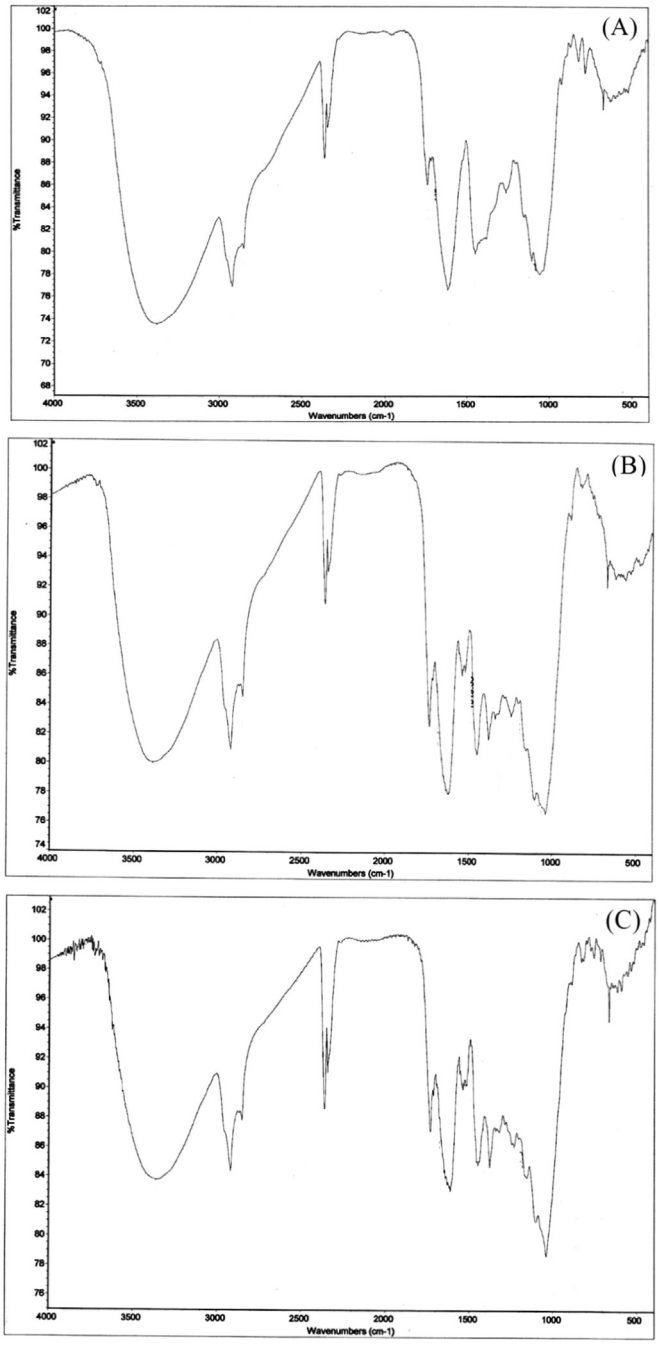

Fig. 1. FTIR spectra of: (A) BPP (B) RB5-loaded BPP and (C) CR-loaded BPP.

(RB5 and CR are anionic dyes in solution for SO_3^- group in their structure). The low adsorption capacity under alkaline conditions could be mainly attributed to that the increasing number of negative charge on the surface of the adsorbent surface could result in electrostatic repulsion between the adsorbent and dye molecules (Aksu and Donmez, 2003). Also the existence of excess OH^- ions in solution may compete with the anionic dyes for the decreasing number of positively charged sites on the adsorbent surface as the pH increased. Hence, the adsorption capacity of BPP at high pH was significantly lower than that at low pH. Several researchers have investigated the effect of pH on adsorption of RB5 and CR by using different types of adsorbents and reported that maximum adsorption occurred in the at pH 3.0 (Yang et al., 2011; Samarghandy et al., 2011).

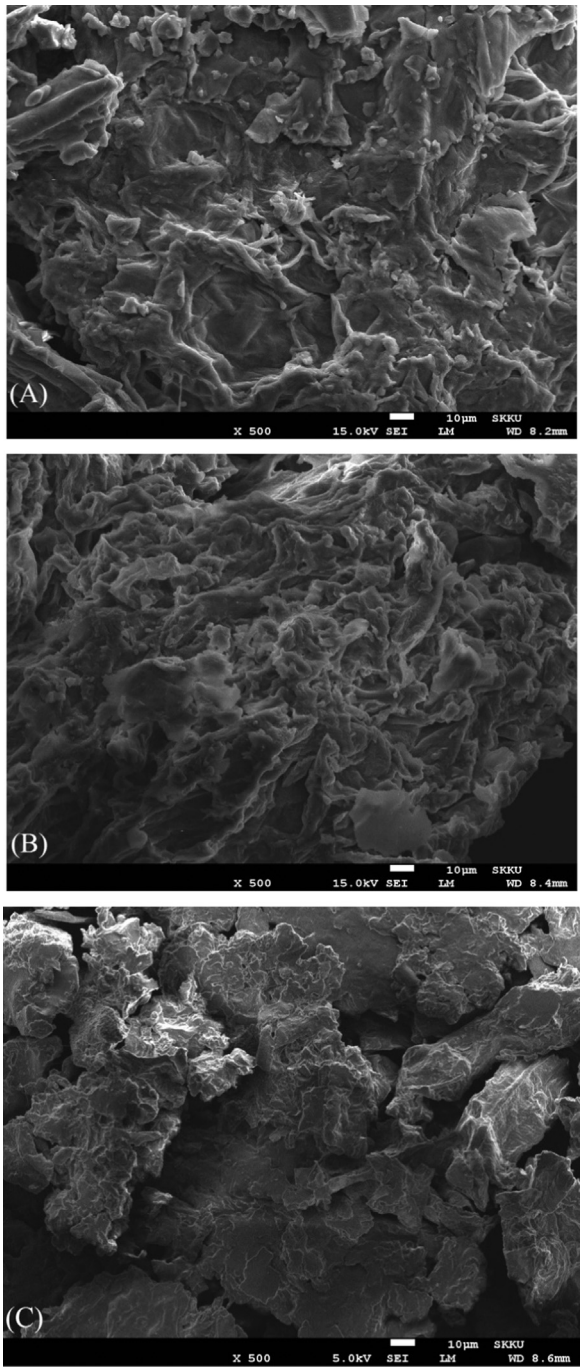

Fig. 2. Scanning electron micrographs of (A) BPP (B) RB5-loaded BPP and (C) CR-loaded BPP.

3.3. Effect of contact time

The effect of contact time on adsorption capacity of BPP for RB5 and CR was investigated at various initial concentrations (50–150 mg/L) and shown in Fig. S1. The adsorption of RB5 and CR occurred very quickly from the beginning of the experiments during the first 60 min, then a slight increase until 180 min where the maximum adsorption of RB5 and CR onto BPP was observed. As contact time increases, dye uptakes also increase initially, and then become almost stable, denoting attainment of equilibrium. This trend in dye uptake may be due to the fact that, initially, all adsorbent sites were vacant and the solute concentration was high. After some period, only a very low increase in the dye uptake was observed because there were few surface active sites on the cell wall of BPP.

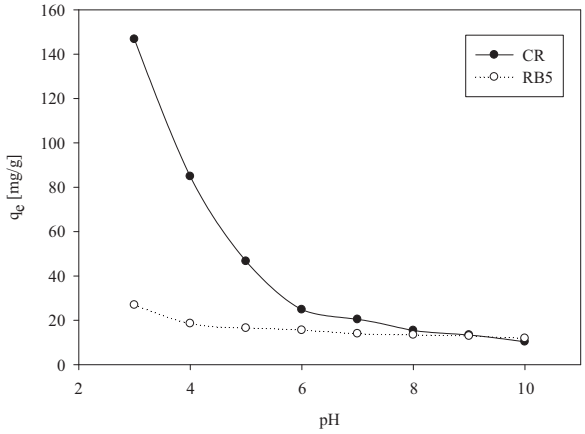

Fig. 3. Effect of pH on the adsorption of RB5 and CR onto BPP.

3.4. Adsorption kinetic study

The adsorption kinetics that describes the solute uptake rate depending on the contact time of the adsorption is one of the important characteristics that define the efficiency of the adsorption. Adsorption kinetics gives important information for designing adsorption systems. In order to investigate the sorption mechanism further, the pseudo-first-order and pseudo-second-order models were used to examine the kinetic data. The two models are generally expressed as follows:

Pseudo-first-order (Lagergren, 1898)

$$q_t = q_1(1 - \exp(-k_1 t)) \quad (4)$$

Pseudo-second-order (Ho and McKay, 1999)

$$q_t = \frac{q_2^2 k_2 t}{1 + q_2 k_2 t} \quad (5)$$

where q_1 and q_2 are the amount of adsorbate adsorbed at equilibrium (mg/g), q_t is the amount of adsorbate adsorbed at equilibrium (mg/g), k_1 is the pseudo-first-order equilibrium rate constant (1/min), and k_2 is the pseudo-second-order equilibrium rate constant (g/mg min). The predicted curves by kinetic models showed good agreement with the kinetics data (Fig. S2 and S3 in supplementary data). The low R^2 values and the difference between q_e and q_1 indicate that the pseudo-first-order model was not well fitted to describe the adsorption of RB5 and CR by BPP. It may be explained that the pseudo-first-order model does not fit well to the whole range of contact time and generally underestimate the q_e values. On the other hand, the R^2 values for the pseudo-second-order model were relatively higher than those of the pseudo-first-order model. Moreover, the q_2 values calculated by the pseudo-second-order model were close to the experimental q_e values. Thus, these results suggest that the pseudo-second-order model provided a good correlation for the adsorption of RB5 and CR onto BPP. The estimated kinetic parameters and correlation coefficients (R^2) from pseudo-first-order and pseudo-second-order models are given in Table 1.

3.5. Adsorption isotherm study

The equilibrium adsorption isotherms are one of the promising data to understand the mechanism of the adsorption. The most commonly applied isotherms, in solid/liquid system, are Langmuir and Freundlich isotherms. The Langmuir equation was chosen for the estimation of maximum adsorption capacity corresponding to complete monolayer coverage on the adsorbent surface. The Freundlich model was chosen to estimate the adsorption intensity of the sorbate on the sorbent surface.

Table 1
Kinetic parameters of pseudo-first-order and pseudo-second-order models for RB5 and CR onto BPP.

Dye	Conc. (mg/L)	q_e (mg/g)	Pseudo-first-order			Pseudo-second-order		
			q_1 (mg/g)	k_1 (L/min)	R^2	q_2 (mg/g)	k_2 (g/mg min)	R^2
RB5	50	10.6	9.94	0.0384	0.8925	11.0	0.0047	0.9836
	100	13.4	12.1	1.0386	0.8122	13.4	0.1527	0.9913
	150	20.0	19.3	0.1625	0.8211	20.1	0.0144	0.9810
CR	50	42.3	41.7	0.9955	0.8793	42.4	0.0455	0.9905
	100	76.2	75.4	1.2317	0.8628	76.2	0.0346	0.9943
	150	115.1	113.9	1.2861	0.9381	115.2	0.0246	0.9950

In this work, attempts have been made to analyze adsorption by these two models. Isotherm plots were drawn for the experimental data of the amount of RB5 and CR adsorbed per unit mass (mg/g) versus equilibrium concentration of RB5 and CR concentration ranging from 50 to 300 mg/L at selected temperatures of 298, 308 and 318 K and the other conditions were kept as constant. The correlation coefficients, R^2 and the Chi-square (χ^2) test were also carried out and calculated to find the best fit among the adsorption isotherm models which has been used. The equation for evaluating the best fit model is to be evolved as:

$$\chi^2 = \sum \frac{(q_e - q_{e,m})^2}{q_{e,m}} \tag{6}$$

where, $q_{e,m}$ is equilibrium capacity obtained by calculating from a model (mg/g), q_e is the experimental data of equilibrium capacity (mg/g).

A basic assumption of the Langmuir theory is that sorption takes place at specific homogeneous sites within the sorbent. This model can be written in non-linear form (Langmuir, 1918).

$$q_e = \frac{q_m K_L C_e}{1 + K_L C_e} \tag{7}$$

where C_e is the equilibrium solute concentration in mg/L, q_e is the amount of adsorbate adsorbed per unit mass of adsorbent in mg/g and K_L is the Langmuir adsorption constant (L/mg) relating the free energy of adsorption. At all the studied temperatures the adsorption capacity of CR on BPP was at least thrice higher than the adsorption capacity of RB5. The value of q_{max} was enhanced and raised from 21.2 to 49.2 mg/g for RB5 and 111.8–164.6 mg/g for CR, respectively, with an increase in the temperature from 298 to 318 K, which could be attributed to a rise in kinetic energy of the sorbent particles due to the rise in temperature. This rise in kinetic energy increases the frequency of collisions between the biosorbent and the sorbate, resulting in enhanced sorption on to the surface of the sorbent.

The essential features of the Langmuir isotherm can be expressed by means of a separation factor or equilibrium parameter R_L is calculated according to the following equation:

$$R_L = \frac{1}{1 + K_L C_o} \tag{8}$$

where K_L is the Langmuir constant (L/mg) and C_o is the initial adsorbate concentration (mg/L). The parameter R_L indicates the shape of the isotherm and nature of the adsorption process ($R_L > 1$: unfavorable; $R_L = 1$: linear; $0 < R_L < 1$: favorable; $R_L = 0$: irreversible). The values of R_L are all in the range of 0–1, which indicate the favorable adsorption of RB5 and CR onto BPP.

The Freundlich model assumes a heterogeneous adsorption surface and active sites with different energy. The Freundlich model (Freundlich, 1906) is

$$q_e = K_f C_e^{1/n} \tag{9}$$

where, K_f (mg/g) and n are the Freundlich constants related to the sorption capacity of the adsorbent and the energy of adsorption respectively. The values of K_f increased from 7.71 to 10.7 mg/g for RB5 and 13.46–15.84 mg/g for CR, respectively, with increase in the temperature of the solution 298–318 K. As the K_f is a measurement of adsorption capacity, the increase in the value again confirms that the adsorption process of RB5 and CR onto BPP is an endothermic process. The *1/n* values are found in the range of 0.17–0.26 for RB5 and 0.37–0.42 for CR, respectively, when the temperature was altered from 298 to 318 K. The *1/n* values between 0 and 1 indicate that the adsorption of RB5 and CR onto BPP is favorable under the conditions studied. The Langmuir and Freundlich correlation coefficients (R^2) and Chi-square (χ^2) values are presented in Table 2.

As can be seen from the isotherms in Fig. S4 and S5 in supplementary data, and regression coefficients in Table 2, the results of the non-linear R^2 and (χ^2) for the two adsorption isotherms indicates that the Langmuir isotherm model appears to be a best fitting model for the adsorption isotherms data of the BPP because it has displayed the highest R^2 and a lowest Chi-square (χ^2) values.

3.6. Comparison of RB5 and CR removal with different adsorbents

The adsorption capacity of BPP for the removal of RB5 and CR has been compared with those of other adsorbents reported in literature and the values of adsorption capacities (q_{max}) have been listed in Table S2. Therefore, it can be noteworthy that the BPP has important potential to removal RB5 and CR from aqueous solution.

3.7. Thermodynamic evaluation

Thermodynamically, in an isolated system, energy cannot be gained or lost; the entropy change is the driving force (Aravindhan et al., 2007). In the practice of environmental engineering, both energy and entropy factors ought to be considered in order to determine the processes that occur spontaneously. Thermodynamic parameters including Gibbs free energy change (ΔG°), enthalpy change (ΔH°) and entropy change (ΔS°) for the adsorption of RB5 and CR onto BPP were calculated using the following equations:

$$\Delta G^o = -RT \ln K \tag{10}$$

where K is the Langmuir equilibrium constant (L/g); R and T represent the universal gas constant (8.314 J/mol K) and the temperature (K).

The enthalpy (ΔH°) and entropy (ΔS°) values were estimated from the following equations:

Table 2
Isotherm parameters for the adsorption of RB5 and CR onto BPP at different temperatures.

Dye	Temp. (K)	Langmuir				Freundlich			
		q_{max}	b	R^2	χ^2	K_f	n	R^2	χ^2
RB5	298	21.2	0.051	0.9994	0.04	7.71	5.76	0.9946	0.3
	308	33.6	0.035	0.9958	0.6	8.5	4.25	0.9818	2.6
	318	49.2	0.033	0.9978	0.6	10.7	3.78	0.9831	5.1
CR	298	111.8	0.024	0.9963	5.1	13.46	2.67	0.9831	23.1
	308	150.1	0.023	0.9964	8.4	15.02	2.41	0.9717	65.7
	318	164.6	0.023	0.9944	15.2	15.84	2.36	0.9666	90.7

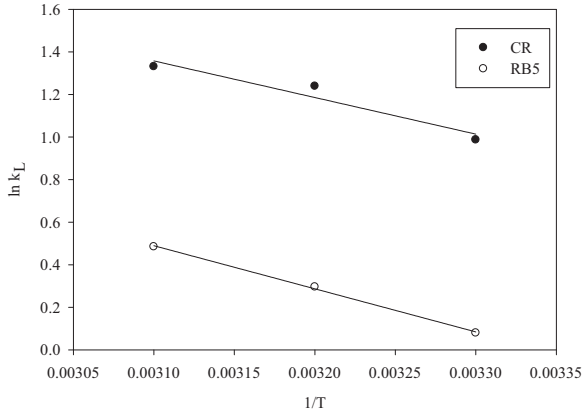

Fig. 4. Plot of ln K vs. 1/T for estimation of thermodynamic parameters for the adsorption of RB5 and CR onto BPP.

Table 3
Thermodynamic parameters for the adsorption of RB5 and CR onto BPP at different temperatures.

Dye	Temp. (K)	ΔG° (kJ/mol)	ΔS° (kJ/mol K)	ΔH° (kJ/mol)
RB5	298	−0.198		
	308	−0.758	0.056	14.15
	318	−1.282		
CR	298	−2.445		
	308	−3.173	0.057	16.84
	318	−3.519		

$$\Delta G^o = \Delta H^o - T\Delta S^o \quad (11)$$

$$\ln K = -\frac{\Delta H^o}{RT} + \frac{\Delta S^o}{R} \quad (12)$$

The values of ΔG° were calculated from Eq. (10). A graph was plotted between reciprocal of temperature (*1/T*) and *ln K*, resulted in a straight line (Fig. 4). The values of ΔH° and ΔS° are evaluated from the slope and intercept of the line. The values of ΔG°, ΔH° and ΔS° for the adsorption of RB5 and CR onto BPP are given in Table 3. The negative values of ΔG° indicate the spontaneous nature of RB5 and CR adsorption onto BPP. Generally, a value of ΔG° in between 0 and −20 kJ/mol is consistent with electrostatic interactions between adsorption sites and the adsorbing ion (physical adsorption) while a more negative values ranging from −80 to −400 kJ/mol indicates that adsorption involves charge sharing or transferring from the adsorbent surface to the adsorbing ion to form a coordinate bond (chemisorption) (AIOthman et al., 2014). As can be seen from Table 3, the magnitude of ΔG° values indicates a typical physical adsorption. The positive values of ΔH° indicate the endothermic nature of the adsorption of RB5 and CR onto BPP in the temperature range of 298–318 K. The magnitude of ΔH° may give an idea about the type of sorption. Two main types of adsorption are physical and chemical. In general, the heat evolved during physical adsorption generally falls into the range of 8–25 kJ/mol, while the heat of chemical adsorption generally falls into the range of 80–200 kJ/mol (Aksu and Karabayir, 2008). Therefore, RB5 and CR adsorption by BPP can be considered as a physical adsorption. The positive values of ΔS° suggested an increase in randomness at the solid/liquid interface during the adsorption of RB5 and CR onto BPP.

3.8. Desorption studies

Regeneration requires proper selection of eluent, which strongly depends on the type of adsorbent and the mechanism of adsorption. The selected eluent must be effective, harmless to the adsorbent, non-polluting and economic. For this purpose, deionized water, 0.1 M HCl, 0.1 M CH_3COOH and 0.1 M NaOH was used as eluents. Fig. S6 shows that the efficiency of the adsorption of RB5 and CR onto BPP after treatment with different eluents. The results show that the CR showed better desorption than RB5 for all the eluents. 0.1 M HCl had minimum efficiency of 21.5% for RB5 and 30.8% for CR, respectively, while it was much better for deionized water (44.8% for RB5 and 56% for CR) and (37.7% for RB5 and 68.7% for CR) for 0.1 M CH_3COOH. But, 0.1 M NaOH eluent can effectively desorbed (95.7% for RB5 and 98% of CR) from adsorbent material.

4. Conclusions

The finding of present study suggests BPP as a suitable adsorbent for CR removal than the RB5 in batch experiments. The batch study parameters; pH of solution, contact time, initial dye concentration and temperature were found to study the adsorption process to a certain extent. Adsorption of RB5 and CR was shown to dependent on the solution pH and the optimum pH value for the better adsorption was found to be 3.0. Adsorption equilibrium data was better described by the Langmuir isotherm model than the Freundlich isotherm model. The monolayer adsorption capacity of BPP for RB5 and CR was found to be 49.2 and 164.6 mg/g, respectively. This indicates BPP removes thrice higher amount of CR than RB5. The SEM images showed that the RB5 and CR were adsorbed on the pores of BPP. FTIR results revealed that hydroxyl, amine and carboxyl functional groups may be responsible for RB5 and CR adsorption. Kinetic studies demonstrated that the mechanism for adsorption of RB5 and CR followed the pseudo-second-order model, which provided the best fit for the experimental data. Desorption studies were carried out using different eluents. The recovery of the RB5 and CR from BPP was found as higher than 90% using 0.1 M NaOH. The calculated thermodynamic parameters exhibited the feasible, endothermic and spontaneous nature of the adsorption of RB5 and CR at 298–318 K. These results therefore suggest that the BPP can be considered as a potential adsorbent for the removal of CR than RB5 from wastewater.

Appendix A. Supporting information

Supplementary data associated with this article can be found in the online version at http://dx.doi.org/10.1016/j.ecoenv.2017.10.075.

References

Ahmaruzzaman, M., Gupta, V.K., 2011. Rice husk and its ash as low-cost adsorbents in water and wastewater treatment. Ind. Eng. Chem. Res. 50, 13589–13613.
AIOthman, Z.A., Habila, M.A., Ali, R., Ghafar, A.A., Hassouna, M.S.E., 2014. Valorization of two waste streams into activated carbon and studying its adsorption kinetics, equilibrium isotherms and thermodynamics for methylene blue removal. Arab. J. Chem. 7, 1148–1158.
Aksu, Z., Donmez, G., 2003. A comparative study on the biosorption characteristics of some yeasts for remazol blue reactive dye. Chemosphere 50, 1075–1083.
Aksu, Z., Karabayir, G., 2008. Comparison of biosorption properties of different kinds of fungi for the removal of Gryfalan Black RL metal-complex dye. Bioresour. Technol. 99, 7730–7741.
Alinsafi, A., Khemis, M., Pons, M.N., Leclerc, J.P., Benhammou, A., Nejmeddine, A., 2004. Electro-coagulation of reactive textile dyes and textile wastewater. Chem. Eng. Process. 44, 461–470.
Allen, S.J., Mckay, G., Porter, J.F., 2004. Adsorption isotherm models for basic dye adsorption by peat in single and binary component systems. J. Colloid Interface Sci. 280, 322–333.
Arami, M., Yousefi Limaee, N., Mohammad Mahmoodi, N., Salman Tabrizi, N., 2005. Removal of dyes from colored textile wastewater by orange peel adsorbent: equilibrium and kinetic studies. J. Colloid Interface Sci. 288, 371–376.
Aravindhan, R., Raghava Rao, J., Unni Nair, B., 2007. Removal of basic yellow dye from aqueous solution by sorption on green alga *Caulerpa scalpelliformis*. J. Hazard. Mater. 142, 68–76.
Carvalho, H.P., Huang, J., Zhao, M., Liu, G., Dong, L., Liu, X., 2015. Improvement of methylene blue removal by electrocoagulation/banana peel adsorption coupling in a batch system. Alexandria Eng. J. 54, 777–786.
Chatterjee, S., Chatterjee, T., Woo, S.H., 2011. Influence of the polyethyleneimine grafting on the adsorption capacity of chitosan beads for Reactive Black 5 from aqueous solutions. Chem. Eng. J. 166, 168–175.

Ciardelli, G., Corsi, L., Marucci, M., 2000. Membrane separation for wastewater reuse in the textile industry. Resour. Conserv. Recycl. 31, 189–197.
Cristovao, R.O., Tavares, A.P.M., Brigida, A.I., Loureiro, J.M., Boaventura, R.A.P., Macedo, E.A., Coelho, M.A.Z., 2011. Immobilization of commercial laccase onto green coconut fiber by adsorption and its application for reactive textile dyes degradation. J. Mol. Catal. B: Enzym. 72, 6–12.
Devaraj, M., Saravanan, R., Deivasigamani, R., Gupta, V.K., Gracia, F., Jayadevan, S., 2016. Fabrication of novel shape Cu and Cu/Cu_2O nanoparticles modified electrode for the determination of dopamine and paracetamol. J. Mol. Liq. 221, 930–941.
Elisandra do Nascimento, G., Campos, N.F., Jose da Silva, J., Bezerra de Menezes Barbosa, C.M., Duarte, M.M.M.B., 2015. Adsorption of anionic dyes from an aqueous solution by banana peel and green coconut mesocarp. Desalin. Water Treat. 1–6.
Freundlich, H.M.F., 1906. Uber die adsorption in Iasugen. J. Phys. Chem. 57, 385–470.
Gong, R.M., Li, M., Yang, C., Sun, Y.Z., Chen, J., 2005. Removal of cationic dyes from aqueous solution by adsorption on peanut hull. J. Hazard. Mater. B121, 247–250.
Gupta, V.K., Nayak, A., 2012. Cadmium removal and recovery from aqueous solutions by novel adsorbents prepared from orange peel and Fe_2O_3 nanoparticles. Chem. Eng. J. 180, 81–90.
Gupta, V.K., Saleh, T.A., 2013. Sorption of pollutants by porous carbon, carbon nanotubes and fullerene-an overview. Environ. Sci. Pollut. Res. 20, 2828–2843.
Gupta, V.K., Agarwal, S., Saleh, T.A., 2011a. Synthesis and characterization of alumina-coated carbon nanotubes and their application for lead removal. J. Hazard. Mater. 185, 17–23.
Gupta, V.K., Jain, R., Nayak, A., Agarwal, S., Shrivastava, M., 2011b. Removal of the hazardous dye-Tartrazine by photodegradation on titanium dioxide surface. Mater. Sci. Eng. C 31, 1062–1067.
Gupta, V.K., Ali, I., Saleh, T.A., Nayak, A., Agarwal, S., 2012a. Chemical treatment technologies for waste-water recycling-an overview. RCS Adv. 2, 6380–6388.
Gupta, V.K., Jain, R., Mittal, A., Saleh, T.A., Nayak, A., Agarwal, S., Sikarwar, S., 2012b. Photo-catalytic degradation of toxic dye amaranth on TiO_2/UV in aqueous suspensions. Mater. Sci. Eng. C 32, 12–17.
Gupta, V.K., Mittal, A., Jhare, D., Mittal, J., 2012c. Batch and bulk removal of hazardous colouring agent Rose Bengal by adsorption techniques using bottom ash as adsorbent. RSC Adv. 2, 8381–8389.
Gupta, V.K., Kumar, R., Nayak, A., Saleh, T.A., Barakat, M.A., 2013. Adsorptive removal of dyes from aqueous solution onto carbon nanotubes: a review. Adv. Colloid Interface Sci. 193–194, 24–34.
Han, R.P., Ding, D.D., Xu, Y.F., Zou, W.H., Wang, Y.F., Li, Y.F., Zou, L.N., 2008. Use of rice husk for the adsorption of Congo red from aqueous solution in column mode. Bioresour. Technol. 99, 2938–2946.
Ho, Y.S., McKay, G., 1999. Pseudo-second order model for sorption processes. Process Biochem. 34, 451–465.
Jain, A.K., Gupta, V.K., Bhatnagar, A., Suhas, 2003. A comparative study of adsorbents prepared from industrial wastes for removal of dyes. Sep. Sci. Technol. 38, 463–481.
Jain, R., Sikarwar, S., 2008. Removal of hazardous dye Congo red from waste material. J. Hazard. Mater. 152, 942–948.
Jain, S., Jayaram, R.V., 2010. Removal of basic dyes from aqueous solution by low-cost adsorbent: wood apple shell (*Feronia acidissima*). Desalination 250, 921–927.
Karthikeyan, S., Gupta, V.K., Boopathy, R., Titus, A., Sekaran, G., 2012. A new approach for the degradation of high concentration of aromatic amine by heterocatalytic Fenton oxidation: kinetic and spectroscopic studies. J. Mol. Liq. 173, 153–163.
Khani, H., Rofouei, M.K., Arab, P., Gupta, V.K., Vafaei, Z., 2010. Multi-walled carbon nanotubes-ionic liquid-carbon paste electrode as a super selectivity sensor: application to potentiometric monitoring of mercury ion(II). J. Hazard. Mater. 183, 402–409.
Lagergren, S., 1898. About the theory of so-called adsorption of soluble substances. K. Sven. Vetensk. Handl. 24, 1–39.
Langmuir, I., 1918. The adsorption of gases on plane surfaces of glass, mics and platinum. J. Am. Chem. Soc. 40, 1361–1403.
Ma, J., Huang, D., Zou, J., Li, L., Kong, Y., Komarneni, S., 2015. Adsorption of methylene blue and Orange II pollutants on activated carbon prepared from banana peel. J. Porous Mater. 22, 301–311.
Mall, I.D., Srivastava, V.C., Agarwal, N.K., Mishra, I.M., 2005. Removal of congo red from aqueous solution by bagasse fly ash and activated carbon: kinetic study and equilibrium isotherm analyses. Chemosphere 61, 492–501.
Mittal, A., Kaur, D., Malviya, A., Mittal, J., Gupta, V.K., 2009a. Adsorption studies on the removal of coloring agent phenol red from wastewater using waste materials as adsorbents. J. Colloid Interface Sci. 337, 345–354.
Mittal, A., Mittal, J., Malviya, A., Gupta, V.K., 2009b. Adsorptive removal of hazardous anionic dye “Congo red” from wastewater using waste materials and recovery by desorption. J. Colloid Interface Sci. 340, 16–26.
Mittal, A., Mittal, J., Malviya, A., Gupta, V.K., 2010a. Removal and recovery of Chrysoidine Y from aqueous solutions by waste materials. J. Colloid Interface Sci. 344, 497–507.
Mittal, A., Mittal, J., Malviya, A., Kaur, D., Gupta, V.K., 2010b. Decoloration treatment of a hazardous triarylmethane dye, Light Green SF (Yellowish) by waste material adsorbents. J. Colloid Interface Sci. 342, 518–527.
Mohammadi, N., Khani, H., Gupta, V.K., Amereh, E., Agarwal, S., 2011. Adsorption process of methyl orange dye onto mesoporous carbon material-kinetic and thermodynamic studies. J. Colloid Interface Sci. 362, 457–462.
Mohammed, R.R., Chong, M.F., 2014. Treatment and decolorization of biologically treated Palm Oil Mill Effluent (POME) using banana peel as novel biosorbent. J. Environ. Manag. 132, 237–249.
Nascimento, G.E., Campos, N.F., Silva, J.J., Barbosa, C.M.B.M., Duarte, M.M.M.B., 2015. Adsorption of anionic dyes from an aqueous solution by banana peel and green coconut mesocarp. Desalin. Water Treat. 1–16.
Ozacar, M., Sengil, I.A., 2005. Adsorption of metal complex dyes from aqueous solution by pine sawdust. Bioresour. Technol. 96, 791–795.
Panswed, J., Wongchaisuwan, S., 1986. Mechanism of dye wastewater color removal by magnesium carbonate-hydrated basic. Water Sci. Technol. 18, 139–144.
Pavan, F.A., Gushikem, Y., Mazzocato, A.S., Dias, S.L.P., Lima, E.C., 2007. Statistical design of experiments as tool for optimizing the batch conditions to methylene blue adsorption on yellow passion fruit and mandarin peels. Dyes Pigments 72, 256–266.
Rajendran, S., Khan, M.M., Gracia, F., Qin, J., Gupta, V.K., Arumainathan, S., 2016. Ce^{3+}-ion-induced visible-light photocatalytic degradation and electrochemical activity of ZnO/CeO_2 nanocomposite. Sci. Rep. 6, 31641.
Sadaf, S., Bhatti, H.N., 2014. Batch and fixed bed column studies for the removal of Indosol Yellow BG dye by peanut husk. J. Taiwan Inst. Chem. Eng. 45, 541–553.
Saeed, A., Sharif, M., Iqbal, M., 2010. Application potential of grapefruit peel as dye sorbent: kinetics, equilibrium and mechanism of crystal violet adsorption. J. Hazard. Mater. 179, 564–572.
Saleh, T.A., Gupta, V.K., 2011. Functionalization of tungsten oxide into MWCNT and its application for sunlight-induced degradation of rhodamine B. J. Colloid Interface Sci. 362, 337–344.
Saleh, T.A., Gupta, V.K., 2012a. Column with CNT/magnesium oxide composite for lead (II) removal from water. Environ. Sci. Pollut. Res. 19, 1224–1228.
Saleh, T.A., Gupta, V.K., 2012b. Photo-catalyzed degradation of hazardous dye methyl orange by use of a composite catalyst consisting of multi-walled carbon nanotubes and titanium dioxide. J. Colloid Interface Sci. 371, 101–106.
Saleh, T.A., Gupta, V.K., 2012c. Synthesis and characterization of alumina nano-particles polyamide membrane with enhanced flux rejection performance. Sep. Purif. Technol. 89, 245–251.
Saleh, T.A., Gupta, V.K., 2014. Processing methods, characteristics and adsorption behavior of tire derived carbons: a review. Adv. Colloid Interface Sci. 211, 93–101.
Samarghandy, M.R., Hoseinzade, E., Taghavi, M., Hoseinzadeh, S., 2011. Biosorption of reactive black 5 from aqueous solution using acid-treated biomass from potato peel waste. Bioresources 6 (4), 4840–4855.
Saravanan, R., Gupta, V.K., Narayanan, V., Stephen, A., 2013a. Comparative study on photocatalytic activity of ZnO prepared by different methods. J. Mol. Liq. 181, 133–141.
Saravanan, R., Gupta, V.K., Prakash, T., Narayanan, V., Stephen, A., 2013b. Synthesis, characterization and photocatalytic activity of novel Hg doped ZnO nanorods prepared by thermal decomposition method. J. Mol. Liq. 178, 88–93.
Saravanan, R., Joicy, S., Gupta, V.K., Narayanan, V., Stephen, A., 2013c. Visible light induced degradation of methylene blue using CeO_2/V_2O_5 and CeO_2/CuO catalysts. Mater. Sci. Eng. C. 33, 4725–4731.
Saravanan, R., Karthikeyan, N., Gupta, V.K., Thirumal, E., Thangadurai, P., Narayanan, V., Stephen, A., 2013d. ZnO/Ag nanocomposite: an efficient catalyst for degradation studies of textile effluents under visible light. Mater. Sci. Eng. C. 33, 2235–2244.
Saravanan, R., Karthikeyan, S., Gupta, V.K., Sekaran, G., Narayanan, V., Stephen, A., 2013e. Enhanced photocatalytic activity of ZnO/CuO nanocomposite for the degradation of textile dye on visible light illumination. Mater. Sci. Eng. C. 33, 91–98.
Saravanan, R., Thirumal, E., Gupta, V.K., Narayanan, V., Stephen, A., 2013f. The photocatalytic activity of ZnO prepared by simple thermal decomposition method at various temperatures. J. Mol. Liq. 177, 394–401.
Saravanan, R., Gupta, V.K., Mosquera, E., Gracia, F., 2014a. Preparation and characterization of V_2O_5/ZnO nanocomposite system for photocatalytic application. J. Mol. Liq. 198, 409–412.
Saravanan, R., Gupta, V.K., Narayanan, V., Stephen, A., 2014b. Visible light degradation of textile effluent using novel catalyst ZnO/γ-Mn_2O_3. J. Taiwan Inst. Chem. Eng. 45, 1910–1917.
Saravanan, R., Prakash, T., Gupta, V.K., Stephen, A., 2014c. Tailoring the electrical and dielectric properties of ZnO nanorods by substitution. J. Mol. Liq. 193, 160–165.
Saravanan, R., Gracia, F., Khan, M.M., Poornima, V., Gupta, V.K., Narayanan, V., Stephen, A., 2015a. ZnO/CdO nanocomposites for textile effluent degradation and electrochemical detection. J. Mol. Liq. 209, 374–380.
Saravanan, R., Gupta, V.K., Mosquera, E., Gracia, F., Narayanan, V., Stephen, A., 2015b. Visible light induced degradation of methyl orange using β-$Ag_{0.333}$ V_2O_5 nanorod catalysts by facile thermal decomposition method. J. Saudi Chem. Soc. 19, 521–527.
Saravanan, R., Khan, M., Gupta, V.K., Mosquera, E., Gracia, F., Narayanan, V., Stephen, A., 2015c. ZnO/Ag/CdO nanocomposite for visible light-induced photocatalytic degradation of industrial textile effluents. J. Colloid Interface Sci. 452, 126–133.
Saravanan, R., Khan, M.M., Gupta, V.K., Mosquera, E., Gracia, F., Narayanan, V., Stephen, A., 2015d. ZnO/Ag/Mn_2O_3 nanocomposite for visible light-induced industrial textile effluent degradation, uric acid and ascorbic acid sensing and antimicrobial activity. RSC Adv. 5, 34645–34651.
Saravanan, R., Sacari, E., Gracia, F., Khan, M.M., Mosquera, E., Gupta, V.K., 2016. Conducting PANI stimulated ZnO system for visible light photocatalytic degradation of coloured dyes. J. Mol. Liq. 221, 1029–1033.
Silva, C.R., Gomes, T.F., Andrade, G.C.R.M., Monteiro, S.H., Dias, A.C.R., Zagatto, E.A.G., Tornisielo, V.L., 2013. Banana peel as an adsorbent for removing atrazine and ametryne from waters. J. Agric. Food Chem. 2358–2363.
Swaminathan, K., Sandhya, S., Carmalin, S.A., Pachhade, K., Subrahmanyam, Y.V., 2003. Decolorization and degradation of H-acid and other dyes using ferrous-hydrogen peroxide system. Chemosphere 50, 619–625.
Wawrzkiewicz, M., Hubicki, Z., 2009. Removal of tartrazine from aqueous solutions by strongly basic polystyrene anion exchange resins. J. Hazard. Mater. 164, 502–509.
Yang, Y., Wang, G., Wang, B., Li, Z., Jia, X., Zhou, Q., Zhao, Y., 2011. Biosorption of Acid Black 172 and Congo Red from aqueous solution by nonviable Penicillium YW 01: kinetic study, equilibrium isotherm and artificial neural network modeling. Bioresour. Technol. 102, 828–834.